Catalysis of CO Electrooxidation at Pt, Ru, and PtRu Alloy. An in Situ FTIR Study

W. F. Lin,[†] T. Iwasita,*[,‡] and W. Vielstich[‡]

Institut für Physik, Universität der Bundeswehr München, Werner-Heisenberg Weg 39, D-85577 Neubiberg, Germany

Received: November 18, 1998; In Final Form: February 1, 1999

A comparative study of CO electrooxidation on different catalysts using in situ FTIR spectroscopy is presented. As electrode materials, polycrystalline Pt and Ru and a PtRu (50:50) alloy are used. The latter is one of the well-known active alloys for CO oxidation. The potential dependence of the band frequencies for the CO stretch indicates the formation of relatively compact islands at pure Pt and Ru, and a loose adlayer structure at the alloy. This loose structure has a positive effect on the rate of oxidative desorption. CO submonolayer coverages are obtained by integrating the absorption bands for CO_2 produced upon oxidation of adsorbed CO. The band intensities measured at Pt, Ru, and PtRu indicate an influence of the substrate on the absorption coefficient of the CO stretch. It is shown that for a correct description of the catalyst properties toward CO electrooxidation, it must be distinguished between bulk and adsorbed CO. In contrast to the statement of most of the recent papers that a PtRu alloy (50:50) is the material with the highest activity for CO oxidation, it is demonstrated and rationalized in the present paper that for bulk CO oxidation pure Ru is the best catalyst.

1. Introduction

The study of CO electrooxidation is of fundamental as well as of practical interest. Adsorbed carbon monoxide exhibits a surface-sensitive behavior which has been evidenced, e.g. by the vibrational properties of the C−O bond, as proved by FTIR spectroscopy.[1,2] Carbon monoxide is consistently found as impurity in gaseous hydrogen derived from steam-reformed hydrocarbons and as a byproduct during the oxidation of small organic molecules at Pt, the oxidation of CO itself constituting one of the main problems in the electrocatalysis of fuel cell reactions.

It was indicated, already in the late 1960s,[3,4] that for the oxidation of CO, PtRu alloys are better catalysts than pure platinum.[5] The necessity of finding CO-tolerant materials for hydrogen electrodes has motivated renewed interest in this system. Recently, Gasteiger et al.[6−9] have studied the electrooxidation of CO, formic acid, and methanol, using UHV-prepared and thus well-characterized PtRu alloys. The authors claim that a PtRu alloy having a 50:50 surface composition presents the *highest* catalytic activity for CO oxidation.[6−9] This result was also found in our laboratory.[10] However, the statement is only valid for adsorbed CO layers. Watanabe and Motoo[11] studied the oxidation of CO in saturated solutions and reported stationary Tafel plots showing the lowest overpotential for pure Ru.

Differential electrochemical mass spectrometry (DEMS) has been applied to study the catalytic properties of electrodeposited PtRu mixtures for the electrooxidation of CO, methanol, formic acid, and ethanol.[12−16] In contrast with the large number of in situ IR studies on CO adsorption at Pt electrodes,[1] there is, to our knowledge, only one IR spectroscopic study (EMIRS) at pure Ru electrodes in CO saturated solution.[17] At PtRu alloys, apart from a FTIR study of the oxidation of saturated CO adlayers,[13] IR spectra obtained during the oxidation of methanol[18] and some CO band intensity data (from methanol and formic acid oxidation) have been shown.[8] Recently, in situ infrared data on CO adsorption at electrodeposited Ru islands on Pt(111) have been reported.[19] The IR literature for CO adsorption and oxidation on Ru and on PtRu alloys is surprisingly scarce, since in situ FTIR spectroscopy is one of the methods that can contribute to the knowledge of the surface state of carbon monoxide on different materials and give valuable information for the interpretation of electrocatalysis data on this system. In the present work, comparative electrochemical measurements at PtRu alloy (50:50), polycrystalline Pt and Ru, as three basic standards, were performed on both adsorbed CO layers and bulk CO. FTIR data on monolayers and submonolayers of adsorbed CO are presented and discussed. On the basis of the new results, a better understanding of the differences in activity between Pt, Ru, and PtRu for adlayer and bulk CO oxidation is rationalized.

2. Experimental Section

Solutions were prepared with Millipore water (>18 MΩ) and 0.1 M $HClO_4$ (Merck) *pro analysis* as supporting electrolyte. Carbon monoxide had a purity grade of 99.997% (Linde). Nitrogen (Linde 99.999%) was used to deaereate the solution and to keep an air-free atmosphere over the solution during the measurements.

Commercial disk-shaped samples of smooth Pt, Ru, and PtRu alloy (50:50) were used as working electrodes. The geometric areas of the surfaces contacting the electrolyte under meniscus configuration were 0.79 cm^2 (Pt), 0.72 cm^2 (Ru), and 0.20 cm^2 (PtRu). The counter electrode was a Pt sheet for the experiments with a Pt working electrode and a graphite rod was the counter electrode with Ru and PtRu working electrodes.

Potentials were measured against a reversible hydrogen electrode (RHE) in the same supporting electrolyte solution. All experiments were performed at room temperature (ca. 22 °C).

[†] Present address: Fritz-Haber-Institut der Max-Plank Gesselschaft, Faraday-Weg 4-6, 14195 Berlin, Germany.

[‡] Present address: Instituto de Química de São Carlos, Universidade de São Paulo, C.P. 780, CEP 13560-970 São Carlos, Brazil.

10.1021/jp984491+ CCC: $18.00
Published on Web 04/03/1999

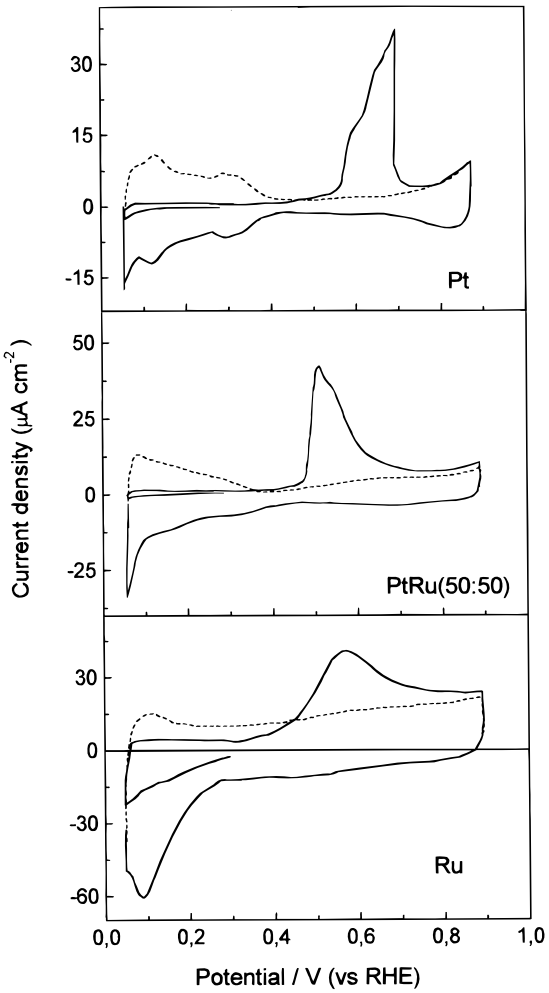

Figure 1. Cyclic voltammograms for the *oxidative stripping* of CO at Pt, PtRu(50:50) alloy, and Ru electrodes in 0.1 M $HClO_4$. The surface was saturated with CO at 0.3 V. After adsorption, CO was displaced from solution by 15 min N_2 bubbling. Sweep rate 0.01 V/s; dashed line: second scan coinciding with the cyclic voltammogram of the clean metal in the supporting electrolyte.

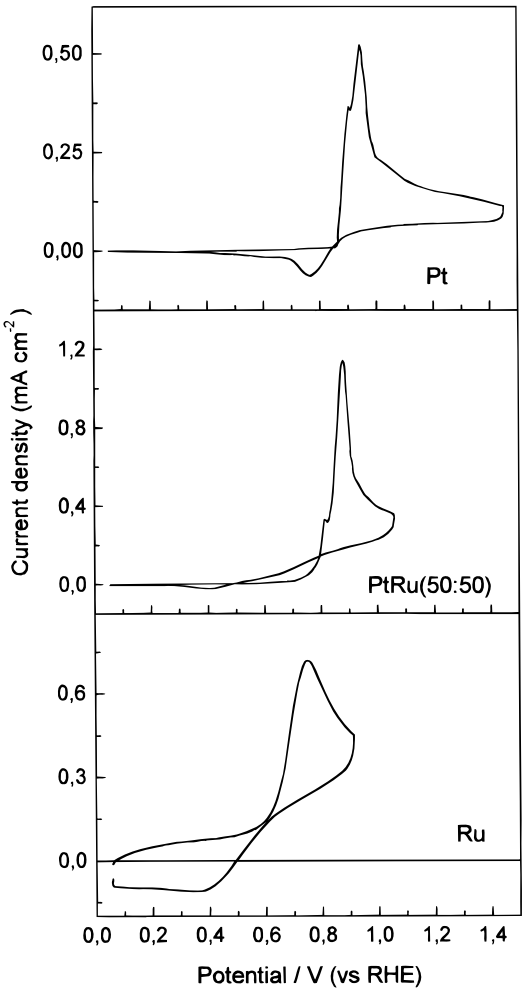

Figure 2. Cyclic voltammograms at Pt, PtRu (50:50), and Ru electrodes in CO-saturated 0.1 M $HClO_4$ solution. Sweep rate 0.05 V/s.

For the FTIR experiments, a Bruker IFS 66 spectrometer equipped with a globar infrared source and a MCT detector was used. The spectroelectrochemical cell, fitted with a 60° CaF_2 prismatic window, was designed as to allow electrolyte exchange under potential control.[18] Except otherwise indicated, for each spectrum 100 interferograms were collected at a resolution of 8 cm^{-1}. Reflectance spectra were calculated as the ratio (R/R_0) of a sample (R) and a reference (R_0) spectrum. Positive and negative going bands represent respectively the loss and gain of species at the sampling potential.

2.1. Experimental Procedure for CO Adsorption. The Pt electrode was flame annealed and cooled in H_2/N_2 atmosphere after which a cyclic voltammogram was obtained in order to control the state of the surface. Ru and PtRu electrodes were polished before each series of measurements in order to get a clean surface having the bulk composition. After polishing, the electrodes were thoroughly rinsed with pure water. No more than three potential cycles between 0.05 and 0.9 V (before Ru dissolution[20]) were applied in order to minimize changes in the surface composition. Carbon monoxide was adsorbed by dosing the gas at a constant potential of 0.3 V vs RHE. For this purpose, CO was directly bubbled, for a very short time, into the solution. Different coverages were then obtained by controlling the adsorption time. Adsorption was interrupted by a rapid exchange of electrolyte using N_2-saturated base solution. During the whole procedure the potential was kept at 0.3 V.

3. Results and Discussion

3.1. Cyclic Voltammetry. After saturation of the surface with CO as described in the preceding section, a potential scan in the range between 0.05 and 0.9 V was applied using a meniscus configuration. The stripping voltammograms for the three electrode materials are shown in Figure 1. Using a sweep rate of 0.01 V s^{-1}, all adsorbed CO was eliminated during the first cycle (full line), the current in a second cycle coinciding with the baseline in the pure supporting electrolyte (dashed line). The respective peak potentials are 0.69 V (Pt), 0.57 V (Ru), and 0.5 V (PtRu). Thus, compared with the pure metals, the alloy exhibits the most negative shift of the peak potential. We observe a sharp onset of current at Pt and PtRu, which contrasts with the sluggish current increase observed at Ru. The onset of current for the Ru sample is observed at ca. 0.3 V. However, as we shall show via FTIR, this is not the value for the onset potential of CO oxidation. These curves compare well with those reported by Gasteiger et al.[6−8] for sputter-cleaned Pt, Ru, and Pt−Ru alloys in sulfuric acid electrolyte and by Krausa and Vielstich[11] for electrodeposited Ru and Pt/Ru on Au substrates.

The electrooxidation of bulk CO out of a saturated electrolyte has been also monitored by cyclic voltammetry. In this case, very different curves and peak potentials are obtained (Figure 2). At a sweep rate of 0.05 V/s, the peak potentials are near

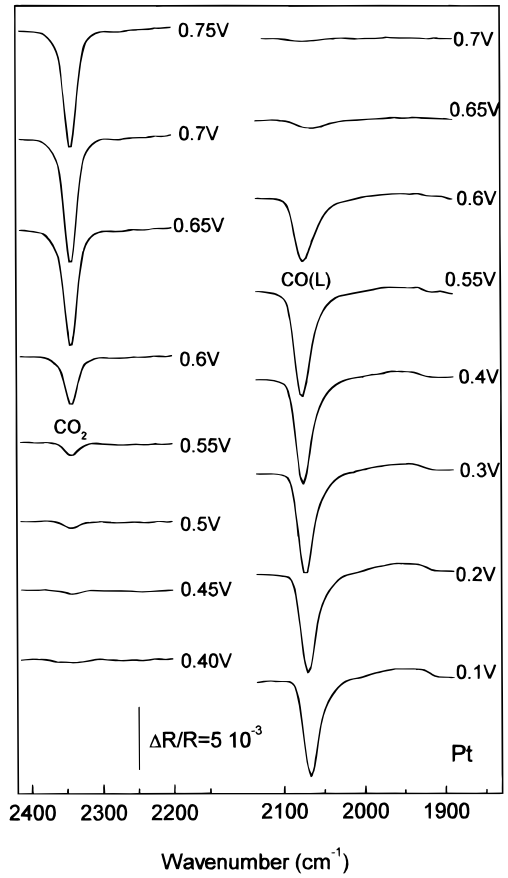

Figure 3. In situ FTIR spectra showing bands for CO adsorbed on Pt and for the CO_2 produced during the CO stripping in 0.1 M $HClO_4$. The CO adlayer was formed as explained in Figure 1. The potential was positively changed from 0.1 V onward in 0.05 V steps. The time elapsed between each step was ca. 30 s. The sample potentials are indicated at the right end of the corresponding spectra. The CO_2 region (band at 2341 cm^{-1}) was calculated with the reference spectrum taken at 0.1 V, a potential where CO_2 is not formed. For the CO region (band near 2070 cm^{-1}) the reference spectrum was one taken at 0.8 V, i.e., a potential where CO_{ads} was completely oxidized.

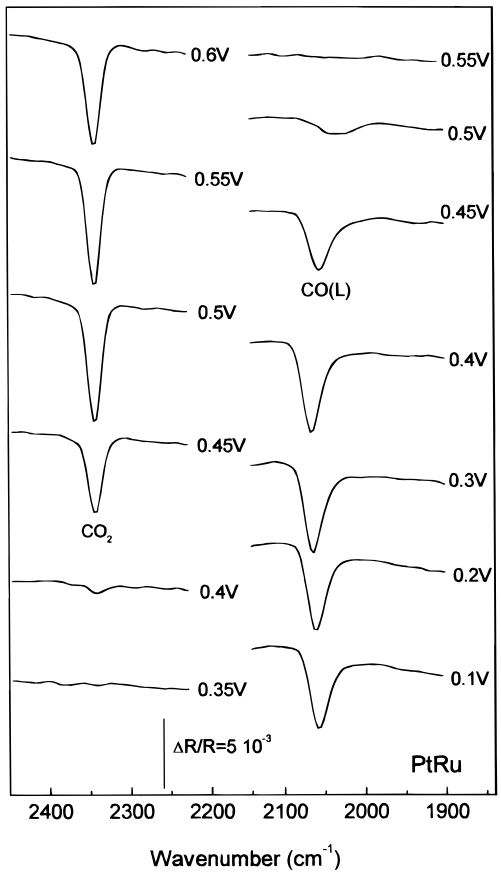

Figure 4. In situ FTIR spectra during the oxidative stripping of CO adsorbed on a PtRu(50:50) alloy electrode in 0.1 M $HClO_4$. Sample potential as indicated. The spectra were obtained and computed as described in Figure 3.

0.95 V for Pt, 0.88 V for PtRu, and 0.73 V for Ru, respectively. Very impressive is the early onset of oxidation on Ru as compared to the other materials. At pure ruthenium, after a more or less constant current at low potentials which is due to a pseudo capacitive process of the surface, oxidation of CO starts and reaches a maximum before the beginning of oxidation at the other two electrodes. This result is in good agreement with early data of Watanabe and Motoo[11] for bulk CO electrooxidation at Pt, Ru, and PtRu catalysts. In the mentioned paper a cathodic shift of the Tafel plots with increasing content in Ru was shown, pure Ru exhibiting the lowest overpotentials.

3.2. In Situ FTIR Spectra. For the in situ FTIR experiments, after CO adsorption at 0.3 V, the potential was stepped to 0.1 V and a series of spectra were taken at subsequently applied potentials in the range 0.1−0.8 V at 0.05 V intervals. Figures 3−5 show the spectra for CO adsorbed at saturation on Pt, PtRu(50:50), and Ru electrodes and for the oxidation product CO_2. The spectra for CO_2 (on the left side of the figures) were calculated against a reference spectrum at 0.1 V, where CO_2 was absent, the increasing negative going bands, showing the formation of CO_2 as the potential is stepped to successively higher potentials. The CO spectra (on the right side of the figures) were calculated taking as a reference a spectrum at 0.8 V, a potential at which CO is completely oxidized and the intensities of the negative-going bands are proportional to the CO coverage at the respective potential.

Only linear bonded CO is observed on the three surfaces. The observed frequencies are 2065−2075 cm^{-1} for Pt, 2055−2065 cm^{-1} for PtRu(50:50), and 2000−2020 cm^{-1} for Ru. The frequency ranges for the CO stretching at pure Pt and PtRu coincide with those reported in the literature for CO at saturation coverage.[13] The value for pure Ru found here is about 15 cm^{-1} lower than that reported by EMIRS measurements in CO saturated 0.5 M $HClO_4$ solution.[17]

3.3. CO Band Intensity and Band Frequency. 3.3.1. General Remarks. The comparison of the potential dependence of the band intensity and band center frequency for adsorbed CO evidences a differential behavior between the three electrode materials under investigation. It should be recalled that, in general, band intensities are affected not only by the total coverage of adspecies. Among the factors affecting the band intensity are changes in the *adsorbate binding geometry*[21] and potential induced *changes of the dipole orientation*, the latter affecting the effective value of the dynamic dipole moment. *Dipole−dipole lateral interactions* can produce a reduction of the dynamic dipole moment.[22] A *Stark effect*[23,24] on adsorbed CO is expected to cause a decrease of the band intensity with increasing positive potentials, at metals where CO is adsorbed through the C-atom as observed for adsorbed CO at Pd(100).[23]

On the other side, the band frequency can increase as the coverage increases due to either dipole−dipole interactions[22] or competition for back-bonding metal electrons. At constant coverage, the band center frequency can shift to higher wavenumbers with increasing potential, either on account of a

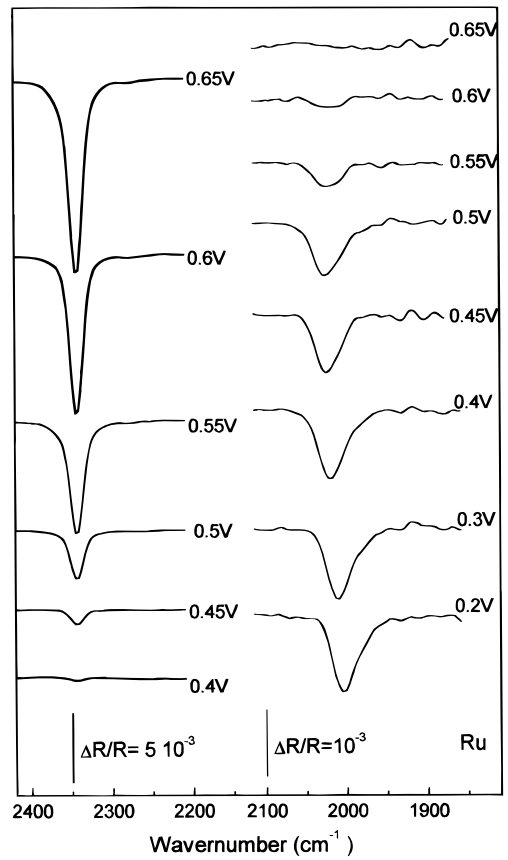

Figure 5. In situ FTIR spectra during the oxidative stripping of CO adsorbed on a Ru electrode in 0.1 M $HClO_4$. Sample potential as indicated. Spectra obtained and computed as in Figure 3.

decreasing back-bonding[25] or as a consequence of the Stark effect on the band frequency.[1,26]

3.3.2. Analysis of the Potential Dependence of Band Intensities and Frequencies. The potential dependence of the band intensities and band frequencies is plotted in Figures 6−8 for Pt, PtRu, and Ru. For Ru and PtRu we observe that the CO band intensity remains constant in the region prior to the onset of oxidation and decreases as the formation of CO_2 begins. For pure platinum the band intensity slightly increases with potential and begin to decrease only 0.1 V behind the onset of CO_2 formation (0.45 V). Similar results were reported by Ianello et al.[13] It should be noted that the data in ref 13 are related to CO adsorbed at 0.07 V (and therefore their voltammogram exhibits a lower onset of CO oxidation with the typical prepeak at 0.45 V[27]) but nevertheless, the reason for the increasing band intensity in our case seems to be the same as that suggested by Ianello et al.[13] At low potentials some CO molecules could lie with their dipole moment vector more or less parallel to the surface and become oriented in the *E* field as the potential increases. The resulting contribution to the average dynamic dipole moment overcompensates the decrease in coverage as the oxidation starts. Since no other features are observed in the spectrum, which could indicate a change in the adsorbate binding geometry, this seems to be a plausible explanation.

All three electrode materials show a different behavior for the potential dependence of the band center (Figures 6−8).

1. For *pure platinum* (Figure 6), the band center exhibits first a linear dependence on potential with $d\upsilon/dE = 28\ cm^{-1}\ V^{-1}$. As CO oxidation starts, υ_{CO} remains approximately constant in the potential interval between 0.45 and 0.55 V and then decreases as the oxidation to CO_2 proceeds.

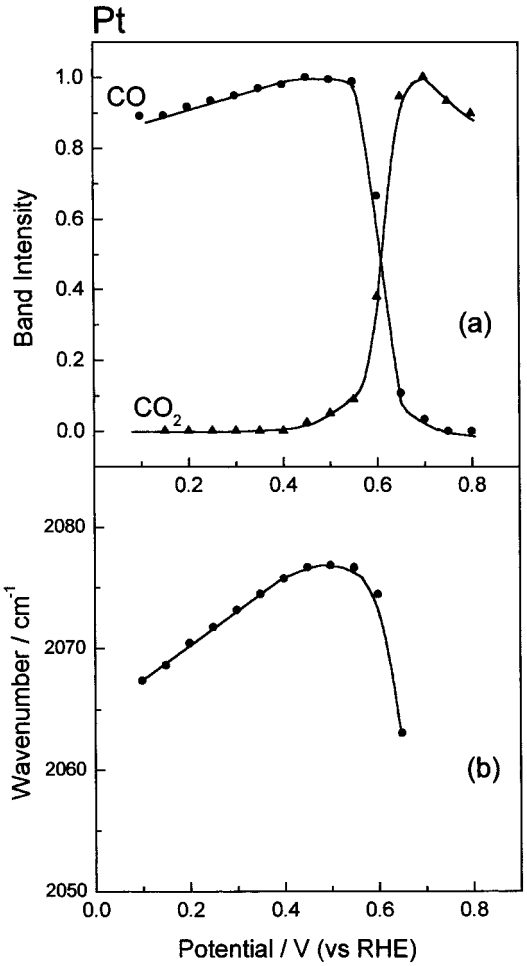

Figure 6. Potential dependence of the band parameters for spectra obtained during CO stripping from a saturated adlayer formed on a Pt electrode at 0.3 V: (a) integrated band intensities for CO_{ads} (circles) and CO_2 (triangles); (b) C−O stretch wavenumber for CO_{ads}. Experimental conditions as in Figure 3. The band intensities were normalized with the maximum value obtained after complete oxidation of CO at 0.8 V.

2. For the *PtRu alloy* (Figure 7), the frequency shifts linearly with $d\upsilon/dE = 32\ cm^{-1}\ V^{-1}$ at low potentials and, as oxidation begins, the frequency drops immediately to lower values.

3. For *pure ruthenium* (Figure 8), the band center frequency shifts linearly up to a potential of 0.25 V with $d\upsilon/dE = 52\ cm^{-1}\ V^{-1}$. Then a more pronounced shift ($d\upsilon/dE$ 77 $cm^{-1}\ V^{-1}$) is observed up to 0.45 V. It should be noted that the onset of oxidation can be extrapolated to 0.4 V, as judged from the CO_2 band intensity.

Thus, *all three materials* differ in their $\upsilon-E$ behavior, particularly in the region of potential close to the start of oxidation. The red shift of the band center frequency for PtRu, which is concomitant with the beginning of oxidation, can be associated to a rapid decrease of the lateral interactions; i.e., it indicates that on this substrate, adsorbed CO presents a relatively *loose adlayer structure*. Contrasting with this, on the pure metals Pt and Ru, CO seems to form somewhat more compact islands. In this case, CO oxidation can occur only at the border of such domains and the local CO coverage remains, at first, relatively high. Here we note also a difference between Pt and Ru. For ruthenium, the blue shift is stronger at potentials above 0.25 V, a potential where the ruthenium urface probably starts being covered with oxide (see below). Thermal desorption data from coadsorption of CO and O at Ru(001) under UHV conditions[28] show a decrease of the CO desorption energy from $E_d = 140$

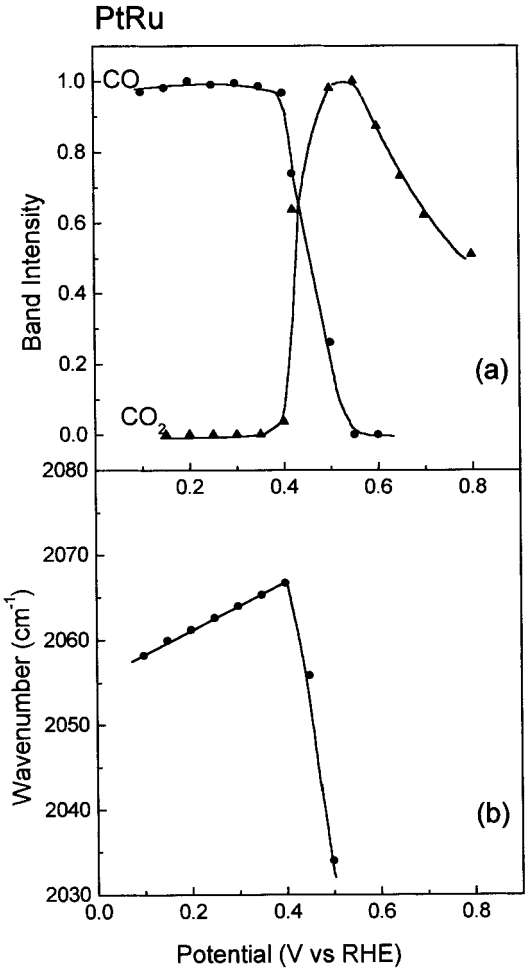

Figure 7. Potential dependence of the band parameters for spectra obtained during CO stripping from a saturated adlayer formed on a PtRu (50:50) electrode at 0.3 V: (a) integrated band intensities for CO_{ads} (circles) and CO_2 (triangles); (b) C−O stretch wavenumber for CO_{ads}. Experimental conditions as in Figure 3. The band intensities were normalized with the maximum value obtained after complete oxidation of CO at 0.8 V.

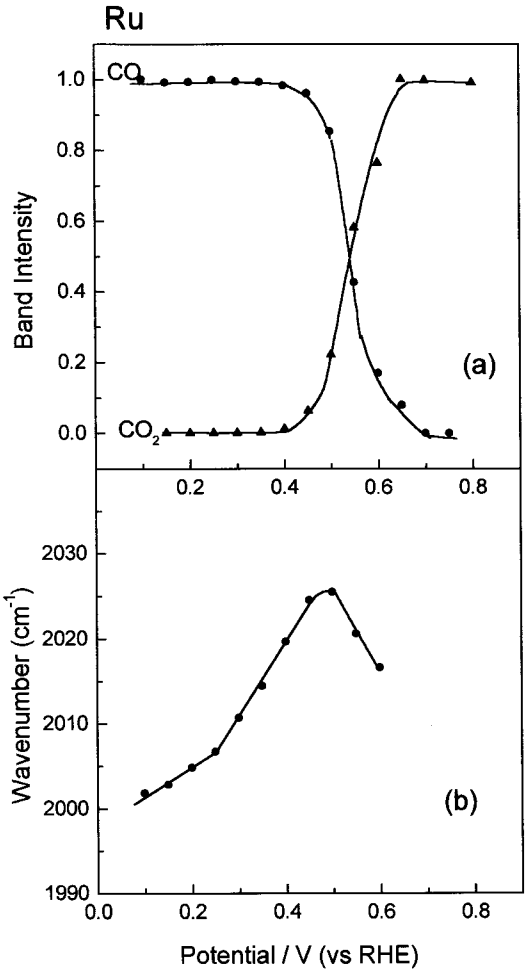

Figure 8. Potential dependence of the band parameters for spectra obtained during CO stripping from a saturated adlayer formed on a Ru electrode at 0.3 V: (a) integrated band intensities for CO_{ads} (circles) and CO_2 (triangles); (b) C−O stretch wavenumber for CO_{ads}. Experimental conditions as described in Figure 3. The band intensities were normalized with the maximum value obtained after complete oxidation of CO at 0.8 V.

kJ mol^{-1} for pure CO adlayers to E_d = 107 kJ mol^{-1} in the presence of coadsorbed oxygen ($\theta_O = 0.5$). Such a behavior is expected in the presence of electronegative coadsorbates, which cause a withdrawal of metal electrons and diminish the metal−π* back-donation. The consequences are a lowering of the metal−CO binding energy as observed in UHV[28] and a stronger C−O bond, which manifests itself in the increase of the υ_{CO} band center between 0.25 and 0.45 V (Figure 7b). It is worth noting that, based on the results of ellipsometric measurements, Ticiannelli et al.[20] suggested a potential of 0.25 V for the formation of adsorbed oxygen at both Ru and PtRu. Data on the effect of oxygen upon the desorption energy of CO_{ad} at PtRu are not available in the literature. In any case, we observe at PtRu only one slope for the υ−E plot in the potential range 0.1−0.4 V.

3.4. Reactivity of Pt, Ru, and PtRu toward Oxidation of CO Adlayers. 3.4.1. CO_2 Formation. As compared to Pt, the onset of CO_2 formation at PtRu and Ru is shifted by about −0.1 and −0.05 V, respectively, Figures 6−8. We also note a faster increase of the CO_2 band intensity for PtRu than for the other materials. Thus, at 0.5 V the CO_2 band intensity reaches already 97% of its maximum value at the alloy and only 23% and 4% of the maximum at Ru and Pt, respectively. A comparison of the cyclic voltammograms for the CO stripping (Figure 1) shows that the current at Ru starts growing faster at around 0.3 V. However, observing that the CO_2 production begins at ca. 0.4 V (Figure 8), we conclude that the onset of current at 0.3 V is not associated with CO oxidation. It could be possible that at this potential some faradaic processes at the Ru surface as, e.g., the formation of Ru(OH), contribute to the observed current.

Comparing the total current changes for the pure metals, after onset of oxidation the reaction occurs at a rather slower rate on Ru (see CV, Figure 1). This behavior was also observed by Gasteiger et al.[6] using stripping voltammetry of saturated CO adlayers. These authors attributed the slower rate observed at Ru to a stronger bonding of OH to Ru than to Pt;[6] according to UHV data, OH desorption energies are 330 kJ mol^{-1} for Ru(001)[29] and 230 kJ mol^{-1} for pure Pt.[30]

3.4.2. Rate of CO Adlayer Oxidation at 0.4 V. From the point of view of technical applications, it can be interesting to test all three materials in respect to the rate of CO oxidation near the onset of CO_2 formation. For this purpose, saturated CO adlayers were prepared by adsorbing CO at 0.3 V. After a potential step to 0.4 V, a series of spectra were obtained in order to observe the change in the CO band intensity with time. The spectra were computed against a reference spectrum obtained at 0.8 V, where the surface becomes free from adsorbed CO. The CO band intensities vs time plots are presented in Figure

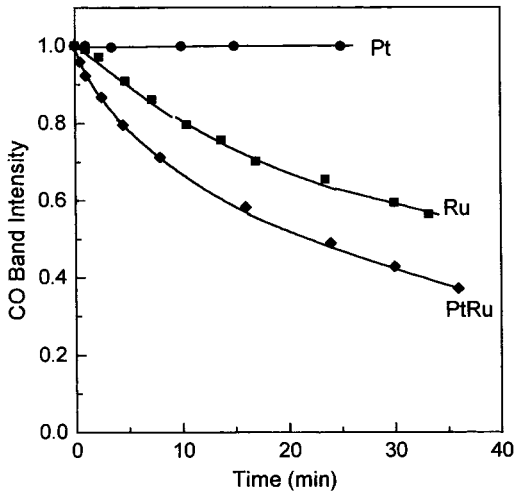

Figure 9. Change of the band intensity for adsorbed CO on Pt, Ru, and PtRu during CO stripping at a constant potential of 0.4 V; spectra (50 scan) were collected each 15 s. The respective surface was saturated with CO at 0.3 V after which, CO was eliminated from the electrolyte by nitrogen bubbling.

9. As expected, the CO band intensity at platinum does not change, since the onset potential for oxidation on this metal lies above 0.4 V. For the other materials we observe the oxidative removal of CO, the rate being higher at PtRu than at pure Ru. It is noteworthy that the same experiment performed at 0.35 V showed CO_2 formation at PtRu after 3 min, while no oxidation was observed at pure Ru even after 10 min. We thus conclude that the onset of oxidation is the lowest on the alloy.

3.5. IR Data at Different CO Coverages. 3.5.1. Degree of Coverage. An interesting insight in the comparative behavior of the three materials used in the present work was accomplished by changing the CO surface coverages, following the dosing procedure described in the experimental part. The CO_2 band intensities for each coverage were normalized with the maximum CO_2 signal, obtained after complete oxidation of a CO_{ad} saturated layer, at 0.8 V. The ratio was taken as a measure for the coverage degree θ_{CO} of the respective electrode. The maximum CO_2 signal was measured at each electrode material by taking several spectra (100 scans each) in order to ensure a complete CO_{ad} oxidation, and to control any diffusion effect of CO_2. Already the first spectrum at 0.8 V exhibited the total loss of CO, the CO_2 intensity remaining unchanged in the two subsequent spectra.

Figure 10 shows in situ FTIR spectra at different CO coverages on Pt, PtRu, and Ru electrodes. It can be seen, i.e., at saturation coverage, that for comparable CO_2 band intensities the corresponding CO_{ad} band intensities largely differ for the three electrodes, the largest signal being observed at Pt and the smallest one at Ru.

3.5.2. Relative Absorption Coefficients of CO on Pt, Ru, and PtRu. For the purpose of comparing the CO band intensity on the different electrode materials, we have normalized the CO band intensities at different coverages, using the corresponding band intensity of the CO_2 produced upon total oxidation of the respective adlayer. The $(CO_{ad})/(CO_2)$ intensity ratios are 0.87 (for Pt), 0.60 (for PtRu), and 0.25 (for Ru). Within the error of integration (ca. 8%), these values are independent of the coverage. Comparing the three CVs of Figure 1, where the current density refers to the respective geometric areas, we can say that the roughness factors of the three electrodes seem to be not very different. This conclusion is supported for the Pt and PtRu electrodes by the almost equivalent CO_2 band

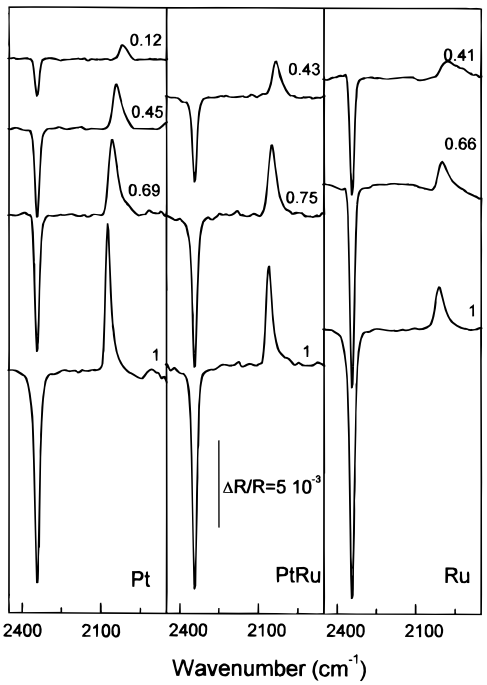

Figure 10. Comparison of in situ FTIR spectra for submonolayer CO adsorbates on Pt, PtRu (50:50), and Ru electrodes in 0.1 M $HClO_4$. Spectra were collected at 0.3 V (i.e., before oxidation of CO_{ads}) and computed against a reference spectrum taken at 0.8 V (after complete oxidation of CO). The CO coverages, indicated on each curve, were calculated as the ratio of the CO_2 band at a given partial coverage and the CO_2 band at saturation coverage.

intensities observed in their spectra (Figure 10). Although the CO_2 intensity is somewhat larger for Ru, the difference with the other metals is not dramatic. Consequently, the normalized intensities of CO_{ad} (referred to the CO_2 production) reflect in a first approximation *the relative values of the absorption coefficient of CO on the three substrates.*

On the basis of the above discussion, the lower intensity of the CO band at Ru may really reflect a lower value for the dynamic dipole moment of the transition on this metal as compared to the other materials. In a study of the effects of coverage on the band intensity and band center of CO_{ad} at Ru(001), Pfnür et al.[31] have suggested that strong dipole−dipole coupling can reduce the dynamic dipole moment. Furthermore, they have shown that this effect markedly depends on the size of the CO islands. Indeed one expects the band intensity to be affected by lateral interactions to a larger extent when adsorption takes place in the form of *large* islands, since in such a case most of CO molecules are surrounded by neighbors of identical nature. Using a different theoretical approach, Persson and Rydberg[22] confirmed the predominance of dipole−dipole coupling in the coverage effects observed by Pfnür et al.,[31] and explained the reduction of the band intensity as being due to a screening effect caused by the electronic polarizability of the adsorbed molecules. If this is the case for Ru in the electrochemical environment, the reduced band intensity for CO adsorbed on this material (Figure 10) could be explained by the existence of strong dipole−dipole coupling and/or large island domains, this being an alternative (or additional) explanation for the lower rate of CO oxidation observed during oxidative stripping at pure ruthenium.

3.5.3. Coverage Dependence of ν_{CO}. The coverage dependence of ν_{CO} for Pt, PtRu, and Ru is shown in Figure 11. A linear dependence of ν_{CO} values is observed for all three materials, the respective $d\nu_{CO}/d\theta_{CO}$ values being 58 cm^{-1} (for

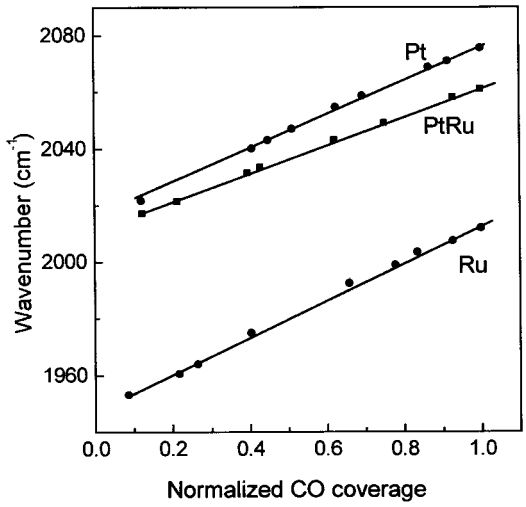

Figure 11. Coverage dependence of the band center frequency for CO_{ads} at Pt, PtRu (50:50), and Ru electrodes in 0.1 M $HClO_4$ at a constant potential of 0.3 V. θ_{CO} was calculated as the ratio of the CO_2 band at a given partial coverage and the CO_2 band at saturation coverage.

Pt), 64 cm^{-1} (for Ru) and 50 cm^{-1} (for PtRu). We can state that, from the spectroscopic point of view, the PtRu (50:50) alloy approaches more closely the behavior of pure Pt than that of pure Ru. For CO produced via methanol adsorption at Pt and PtRu (85:15) somewhat higher frequencies for the alloy than for pure Pt were observed in our group.[18] In that case, the signals were compared on the basis of the band intensities as a measure for the coverage, under the approximation of the same absorption coefficient for both materials.[18] This assumption is not supported by the present results.

3.6. General Discussion of the Proposed Reaction Models. The results in Figures 1 and 2 clearly indicate that for discussing the electrocatalysis of CO electrooxidation, one has to consider that adsorbed CO monolayers and bulk CO molecules represent two different situations in respect to the ease of oxidation. During CO stripping from a monolayer, an increasing amount of free surface sites is available for the dissociation of water, which is the reaction partner in CO oxidation. On the contrary, in the presence of CO in the electrolyte, a continuous supply of CO can keep the surface blocked to a high degree, water dissociation being thus severely hindered. According to the present data and earlier literature results, we can summarize the relevant facts for a reaction model as follows.

(i) CO Stripping vs Bulk CO Oxidation. The results in Figure 1 clearly indicate, that from all three studied materials, the PtRu alloy is the best one for the oxidation of CO out of a monolayer. This result is in good agreement with that of Gasteiger et al.[6,9] According to the IR results we can state that the onset for CO stripping decreases in the order Pt > Ru > PtRu.

On the other hand, Figure 2 shows that ruthenium is the best catalyst for the electrooxidation in the presence of bulk CO, in good agreement with the early result of Watanabe and Motoo.[11] The current for bulk CO oxidation up to a potentials near 0.8 V increases in the order Pt < PtRu ≪ Ru.

(ii) Strength of the Metal−CO Binding. Thermal desorption data on emersed polycrystalline Pt electrodes covered with a monolayer of CO show two desorption states at 420 and 560 K, with a higher population of the high temperature state.[10] Identical experiments on PtRu alloys indicate the inverse situation favoring desorption from the lower state. On the basis of these results, the average Me−CO bond strength decreases in the sequence Pt > PtRu(75:25) > PtRu(50:50].[10]

Respective data for polycrystalline Ru are not available. It was pointed out that at intermediate coverages the bond strength Pt−CO and Ru−CO do not differ very much.[6] However, in the presence of adsorbed O the binding of CO to Ru is markedly weakened.[28] This can also be the case in the electrochemical environment, as shown by the pronounced frequency shift at Ru as the formation of OH begins (section 3.3, Figure 8). We could, in principle, take this fact as an indication of a weaker metal−CO binding for Ru as compared to Pt, at least in the presence of adsorbed OH.

(iii) Strength of the Metal−O Binding. Watanabe and Motoo[11] have observed that, at open circuit potential, dissolved oxygen can remove adsorbed CO from Ru, but not from Pt electrodes. This result is in agreement with a weaker metal−CO bond at Ru, as discussed in (ii) and/or a stronger binding of oxygen to Ru than to Pt as indicated by UHV data.[29,30] These facts give a basis to the currently accepted statement that dissociation of water occurs on Ru at lower potentials than at Pt. In other words, water preferentially dissociates at Ru as compared to Pt. Let us recall that the onset of current at the Ru electrode (Figure 1c) is related with a pseudofaradaic process at the surface and not with CO oxidation, as explained in section 3.4. For the PtRu system, Watanabe and Motoo[11] suggested the so-called Ru oxide to be Ru(OH), formed according to

$$Ru + H_2O \rightarrow Ru(OH) + H^+ + e^- \qquad (1)$$

Frenlink et al. assumed the formation of a ruthenium oxide RuO,[32] but no definite proofs of the nature of the surface species have been given and for the present discussion the real nature of the oxide is irrelevant.

(iv) At Pt and Ru, CO forms relatively compact islands. In contrast, PtRu surfaces present a loose CO adlayer structure, as proved by the potential/frequency shifts at the onset of CO oxidation (section 3.3, Figures 6−8).

3.6.1. Oxidation of CO Monolayers and Submonolayers. In the course of CO oxidation from an adsorbed layer, free surface sites are formed, where water molecules can adsorb and dissociate, e.g., according to reaction 1. In the absence of CO in the bulk of the solution, water does not need to compete for adsorption sites. Thus, in our opinion, an important condition for oxidation is that the CO adlayer presents a *loose structure* where Ru(OH) can be formed in the immediate vicinity of adsorbed CO molecules.

For the pure metals, our results indicate the formation of island structures. The strong lateral interactions at Ru (dipole−dipole coupling) may be the reason for a slower stripping rate at this metal as compared to Pt, although Ru presents an earlier onset of reaction and that the Ru−CO bond is probably weakened as the formation of oxide begins.

In the case of the alloy, there are at least two reasons for the better catalytic behavior toward CO stripping. One is the lowering of the average metal−CO binding as proved by TDS, and the second is the formation of a loose adlayer structure as demonstrated by the band center shift in Figure 7. The reaction steps on the alloy can thus be written as follows:

$$Ru + H_2O \rightarrow Ru(OH) + H^+ + e^- \qquad (1)$$

$$Ru(OH) + Pt{-}CO \rightarrow CO_2 + H^+ + e^- \qquad (2a)$$

$$Ru(OH) + Ru{-}CO \rightarrow CO_2 + H^+ + e^- \qquad (2b)$$

3.6.2. CO Bulk Oxidation. In the case of bulk CO oxidation out of a saturated solution, H_2O molecules have to compete for

each place free of adsorbate, with a continuous supply of CO from the solution. If, as stated above, CO is bonded more strongly to Pt than to Ru, Pt atoms will be steadily poisoned against OH formation and, under these conditions, a maximum in Ru concentration at the surface must represent the optimum situation for CO oxidation. Even having a relatively low rate for the oxidation of adsorbed CO, pure ruthenium is, from all three materials, the best catalyst for bulk CO oxidation because it is less poisoned in the presence of CO in the bulk of the solution. The onset of CO_{ad} oxidation at pure Ru is ca. 0.05 V more anodic than at PtRu; nevertheless, the advantage of Ru of being less poisoned prevails and, even presenting a less steep increase in current as compared with Pt and PtRu, the voltammogram for Ru reaches the maximum *before* the onset of oxidation on the other materials. The reaction sequence is

$$Ru + H_2O \rightarrow Ru(OH) + H^+ + e^- \quad (1)$$

$$Ru(OH) + Ru{-}CO \rightarrow CO_2 + H^+ + e^- \quad (2b)$$

4. Concluding Remarks

The results presented here stress the differences between both oxidative stripping and bulk CO electrooxidation. These differences are deciding in the search for CO-tolerant electrode materials. When bulk CO is present, pure ruthenium is the most active catalyst. Near adsorbed OH a weakening of the Ru−CO binding can be inferred from the increase of the ν_{CO} band center shift $d\nu/dE$ at potentials above 0.25 V.

A comparison of the CO_{ad}/CO_2 intensity ratio at saturated coverage indicates that the values of the absorption coefficient for CO adsorbed at polycrystalline Pt, Ru and PtRu alloy(50:50) vary in the order Pt > PtRu > Ru.

Infrared spectroscopy data indicate that the surface structure of the CO adlayer strongly differs for Pt, PtRu, and Ru. The pure metals present a relatively compact adlayer structure while the alloy exhibit a loose CO_{ad} structure thus offering the best distribution of CO_{ad}/OH_{ad} reactive pairs. This justifies the finding in the literature that a 50:50 PtRu alloy presents the best reactivity toward CO_{ad} oxidation.

Acknowledgment. W.F.L. acknowledges the Alexander von Humboldt-Stiftung for a Research Fellowship. Financial support from the Deutsche Forschungsgemeinschaft and the Fonds der Chemischen Industrie is gratefully acknowledged.

References and Notes

(1) Iwasita, T.; Nart, F. C. In *Advances in Electrochemical Science and Engineering*; Gerischer, H., Tobias, Ch., Eds.; Verlag Chemie; Weinheim, FRG, 1995; Vol. 4, p 123.
(2) Chang, S-C.; Weaver, M. *Surf. Sci* **1990**, *238*, 142.
(3) Niedrach, L. W.; McKee, D. W.; Paynter, J.; Danzig, I. F. *Electrochem. Technol.* **1967**, *5*, 318.
(4) McKee, D. W.; Scarpellino, A. J. *Electrochem. Technol*. **1968**, *6*, 101.
(5) Ross, P. N.; Kinoshita, K.; Scarpellino, A. J.; Stonehart, P. *J. Electroanal. Chem.* **1975**, *63*, 97.
(6) Gasteiger, H. A.; Markovic, N.; Ross, P. N.; Cains, E. J. *J. Phys. Chem.* **1994**, *98*, 617.
(7) Gasteiger, H. A.; Markovic, N.; Ross, P. N.; Cains, E. J. *Electrochim. Acta* **1994**, *39*, 1825.
(8) Markovic, N.; Gasteiger, H. A.; Ross, P. N.; Jiang, X.; Villegas, I.; Weaver, M. J. *Electrochim. Acta* **1995**, *40*, 91.
(9) Gasteiger, H. A.; Markovic, N. M.; Ross, P. N. *J. Phys. Chem*. **1995**, *99*, 8220.
(10) Iwasita, T.; Dalbeck, R.; Pastor, E.; Xia, X. *Electrochim. Acta* **1994**, *39*, 1817.
(11) Watanable, M.; Motoo, S. *J. Electroanal. Chem.* **1975**, *60*, 275.
(12) Krausa, M.; Vielstich, W. *J. Electroanal. Chem.* **1994**, *379*, 307.
(13) Ianniello, R.; Schmidt, V. M.; Stimming, U.; Stumper, J.; Wallau, A. *Electrochim. Acta* **1995**, *39* 1863.
(14) Lin, W. F.; Xia, X. H.; Vielstich, W. *International Meeting on Surface Electrochemistry*; Alicante, Sept. 7−10, 1997; Abstract P40.
(15) Souza, J.; Rabelo, F.; Moraes, I.; Nart, F. C. *J. Electroanal. Chem.* **1997**, *420*, 17.
(16) Schmidt, V. M.; Ianniello, R.; Pastor, E.; Gonzalez, S. *Phys. Chem*. **1996**, *100*, 17901.
(17) Gutierrez, C.; Caram, J. A.; Beden, B. *J. Electroanal. Chem.* **1991**, *305*, 289.
(18) Iwasita, T.; Nart, F. C.; Vielstich, W. *Ber. Bunsen-Ges. Phys. Chem.* **1990**, *94*, 1030.
(19) Friedrich, K. A.; Geyzers, K. P.; Linke, U.; Stimming, U.; Stumper, J. *J. Electroanal. Chem.* **1996**, *402*, 123.
(20) Ticiannelli, E.; Berry, J. G.; Paffet, M. T.; Gottesfeld, S. *J. Electroanal. Chem.* **1989**, *258*, 61.
(21) Kitamura, F.; Takahashi, M.; Ito, M. *Surf. Sci.* **1989**, *223*, 493.
(22) Persson, B. N. J.; Rydberg, R. *Phys. Rev. B* **1981**, *24*, 6954.
(23) Lambert, D. K. *J. Chem. Phys.* **1991**, *94*, 6237.
(24) Nart, F. C.; Iwasita, T. *Electrochim. Acta* 1996, *41*, 631.
(25) Blyholder, G. *J. Phys. Chem.* **1964**, *68*, 2772.
(26) Lambert, D. K. *Electrochim. Acta* **1996**, *41*, 623.
(27) Iwasita, T.; Vogel, U. *Electrochim. Acta* **1988**, 33, 557.
(28) Madey, T. E.; Benndorf, C. *Surf. Sci.* **1985**, *164*, 602.
(29) Madey, T. E.; Engelhardt, A. H.; Menzel, D. *Surf. Sci.* **1975**, *48*, 304.
(30) Campbell, C. T.; Ertl, G.; Kuipers, H.; Segner, J. *J. Chem. Phys.* **1980**, *73*, 5862.
(31) Pfnür, H.; Menzel, D.; Hoffmann, F. M.; Ortega, A.; Bradshaw, A. M. *Surf. Sci.* **1980**, *93*, 431.
(32) Frelink, T.; Visscher, W.; van Veen, J. A. R. *Langmuir* **1996**, *12*, 3702.